Data-Driven Gas Sensing Performance of Cdo Thin Films

Hiba Saad Rasheed[1], Ibtihaj Shukur Abdulfattah[2], Maryam Ahmed Sabri[2], Muhaned Zaidi[3] and Israa Akram Abbas[1]

[1]*Department of Physics, College of Education, Mustansiriyah University, 10052 Baghdad, Iraq*
[2]*Division of Human Resources, Mustansiriyah University Presidency, 10052 Baghdad, Iraq*
[3]*Department of Medical Physics, College of Science, Al-Manara University, 62001 Amarah, Iraq*
hibasaad@uomustansiriyah.edu.iq, eshkor83@uomustansiriyah.edu.iq, mariamahmed.ma754@gmail.com, muhanedzaidi@uomanara.edu.iq, ssaakk02@uomustansiriyah.edu.iq

Keywords: Cdo, Thickness, SP Method, Structural Properties, Morphological, Optical, Energy Gap, Sensitivity.

Abstract: This study explores how different film thicknesses (250, 300, and 350 nm) of CdO thin films deposit by spray pyrolysis (SP). XRD analysis confirmed the polycrystalline nature, demonstrating a preference for direction towards the (200) plane. Crystallite size increased with thickness. AFM analyses revealed a reduction in surface roughness and grain size with increased thickness, indicating smoother, more uniform films. Optical analysis showed a decrease in both absorbance and bandgap energy (from 2.58 eV to 2.43 eV) as the film thickness increased, due to improved crystallinity and sub-level formation in the band structure. Both extinction coefficient and refractive index exhibited a decline as the film thickness increased, indicating enhanced optical quality and reduced surface defects. Gas sensing performance was evaluated using NO_2 gas. Thinner films (250 nm) exhibited higher sensitivity due to greater surface area and more active adsorption sites. Sensitivity significantly decreased with increased thickness due to a reduced surface-to-volume ratio.

1 INTRODUCTION

CdO is a material that has the potential to be employed as a transparent semiconductor due to its high optical transmittance in the visible area [1]-[4]. heat mirrors, and gas sensors are among the numerous uses of CdO [5]-[11]. Multiple fabrication methods were adopted to deposit CdO thin films on various bases, including metalorganic chemical bath deposition [9]-[14]. SILAR [10]-[12], SP method [13], [14] vacuum evaporation [15], [16], PLD [17], [18], magnetron sputtering [19], reactive evaporation [20], [21], chemical vapor deposition [22], [23], radio frequency magnetron sputtering [24] and spin coating technique [25], [26]. Among these methods, SP stands out due to its advantages of simplicity, operational safety, and cost-effectiveness in both equipment and precursor materials. In this method, the precursor solution is sprayed onto a heated substrate using a carrier gas-assisted nozzle. The thermally induced decomposition of the droplets upon impact results in thin film formation [14]. In this study, CdO thin films were deposited using SP technique, with the primary objective of examining their physical properties.

2 EXPERIMENTAL

The implemented spray pyrolysis coating system produced uniform CdO thin confirming the system's deposition capabilities. The precursor solution was prepared from 0.1 M $CdCl_2$ dissolved in a 1:1 mixture of redistilled water and ethanol. To ensure solution homogeneity, several drops of hydrochloric acid (HCl) were introduced, with the total sprayed precursor volume maintained at 50 ml throughout the deposition process. The preparation process employed the following parameters: the substrate was heated to 450°C, and a distance of 29 cm was maintained between spout and substrate to prevent cooling. The deposition was performed at a constant spray rate of 5 ml/min, utilizing N_2 as the carrier gas to ensure thermal stability throughout the process. Film thickness determination via gravimetric analysis yielded a value of 340 ± 20 nm. XRD analysis was employed to conduct structural evaluation, with

complementary surface morphological evaluation conducted via AFM. Optical properties were systematically investigated through transmittance and absorption spectroscopy measurements performed with a dual-beam. For optical characterization, transmission and absorption properties were measured using a computer-controlled double-beam spectrophotometer covering 300-900 nm wavelength range.

3 RESULTS AND DISCUSSIONS

The implemented spray pyrolysis coating system produced uniform cadmium oxide thin films, confirming the efficiency of the deposition process. The precursor solution was prepared from cadmium chloride at 0.1 molar concentration dissolved in a 1:1 mixture of distilled water and ethanol. To improve solution homogeneity, a few drops of hydrochloric acid were added, while the total sprayed volume was kept constant at 50 milliliters during deposition.

The substrate temperature was maintained at 450°C, and a fixed distance of 29 cm was kept between the spray nozzle and the substrate to avoid unwanted cooling effects. The deposition was carried out at a constant spray rate of 5 ml per minute using nitrogen as a carrier gas to ensure thermal stability. The film thickness determined by gravimetric analysis was 340 ± 20 nm. Structural analysis was performed using X-ray diffraction, while surface morphology was examined by atomic force microscopy. Optical properties were studied using transmittance and absorption measurements in the wavelength range from 300 to 900 nm using a dual-beam spectrophotometer.

Figure 1 shows the X-ray diffraction patterns of the prepared cadmium oxide films. All samples with thicknesses between 250 and 350 nm exhibit characteristic diffraction peaks at 33.08°, 38.32°, 55.36°, and 65.89°, corresponding to the (111), (200), (220), and (311) crystal planes of cubic cadmium oxide (JCPDS card No. 05-0640). The most intense peak at 38.32° indicates a preferred orientation along the (200) plane, consistent with previous studies [17].

The crystallite size was calculated using the Scherrer approach [27], [28]. The results show that the crystallite size increases with film thickness from 10.90 nm to 12.75 nm [29], [30]. This increase is attributed to a reduction in nucleation sites at higher thickness, allowing existing grains to grow larger. As the film becomes thicker, fewer nucleation centers form, which promotes grain growth around existing nuclei and results in coarser microstructures.

The dislocation density, defined as the inverse square of crystallite size, decreases with increasing thickness from 84.16 to 61.51, indicating improved crystalline quality and reduced defect concentration [31], [32], [33], [34]. Similarly, the microstrain decreases from 27.19, suggesting a gradual relaxation of lattice distortions [35], [36]. The structural parameters are summarized in Table 1, while the variation of crystallite size and peak broadening is illustrated in Figure 2. Overall, the reduction in dislocation density and strain with increasing thickness confirms improved crystal quality and better atomic ordering in thicker films [15], [37].

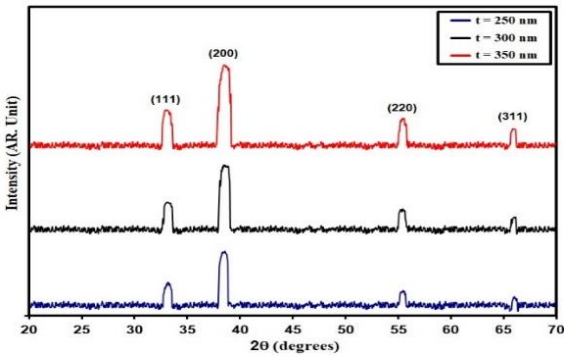

Figure 1: XRD patterns of the synthesized films.

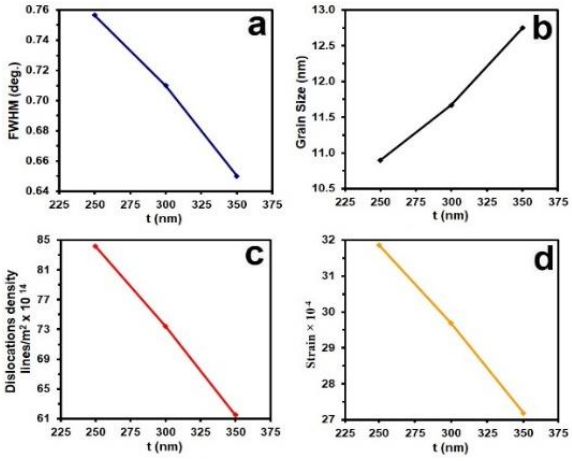

Figure 2: S_{par} of the grown films.

Figure 3 offers AFM topographic images of deposited films at different thicknesses. The micrographs demonstrate high-quality surface morphology characterized by uniformly distributed pyramidal structures across the entire substrate area. The increase in the prominence of this pyramidal structure indicates an improvement in both crystallinity and surface roughness as the doping content increases. AFM analysis revealed a clear

inverse relationship between film thickness and particle size (P_s), with measured values of 83.2 nm (250 nm thickness), 63.9 nm (300 nm), and 41.6 nm (350 nm). Additionally, the average surface roughness (Ra) values increased from 3.19 nm to 16.6 nm, while the root mean square (RMS) roughness values rose from 4.81 nm to 10.19 nm with increasing thickness. This enhancement in surface roughness (Ra) is beneficial for applications such as solar cells and photodetectors, as it can improve light absorption and charge carrier interactions. The AFM parameters (A_{par}) versus film thickness are shown in Figure s 3(a3), 3(b3), and 3(c3), and the corresponding numerical values are listed in Table 2. This data suggests that controlling thickness and doping level effectively tunes the surface morphology, directly influencing the films' functional performance [38].

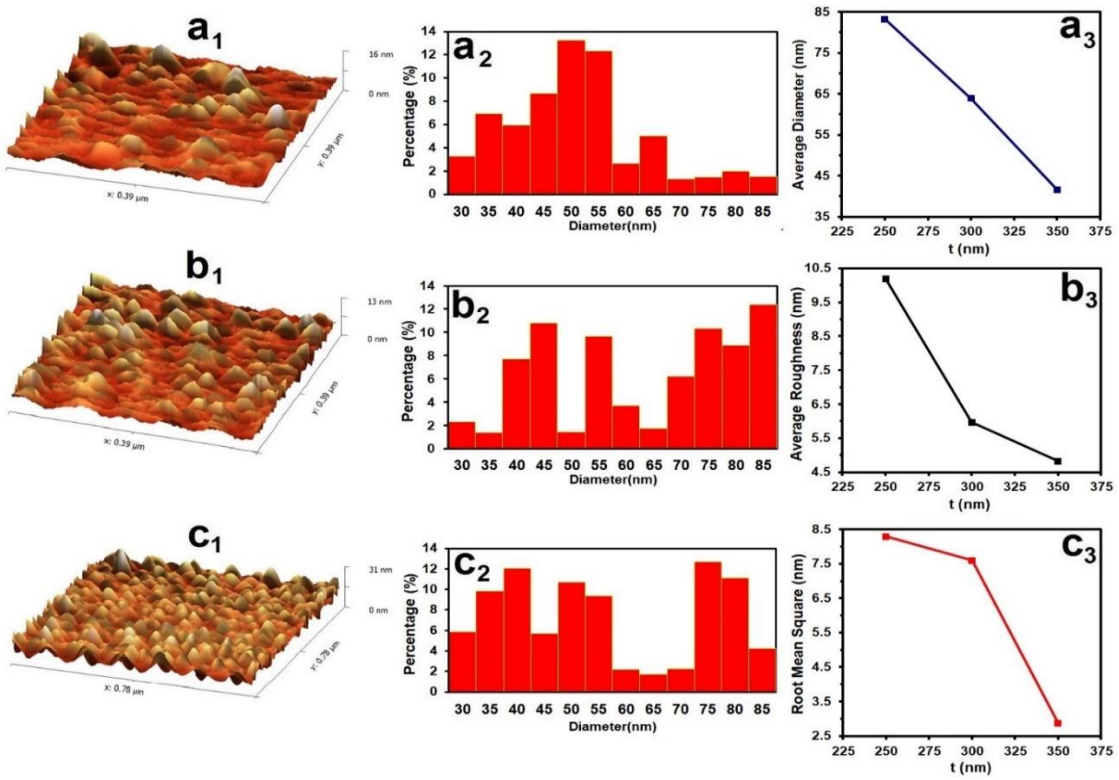

Figure 3: AFM topographic images of deposited films at different thicknesses.

Table 1: *D*, E_g, and S_{par} of the deposited CdO films.

Sample	2 θ (º)	(hkl) Plane	FWHM (º)	E_g (eV)	*D* (nm)	δ (× 10^{14}) (lines/m^2)	ε (× 10^{-4})
250 nm	33.08	200	0.75	2.58	10.90	84.16	31.86
300 nm	33.04	200	0.71	2.52	11.67	73.42	29.69
350 nm	33.00	200	0.65	2.43	12.75	61.51	27.19

Table 2: A_{par} of the synthesized films.

Sample (nm)	P_s (nm)	R_a (nm)	RMS (nm)
250	83.2	10.19	8.29
300	63.9	5.97	7.60
350	41.6	4.81	2.87

The optical characterization was performed across the 300-900 nm wavelength range. Figure 4 shows the absorbance spectra, revealing distinct absorption features that vary with film thickness, all deposited films (250-350 nm thickness range) demonstrated reduced absorbance (A) in the visible spectrum's short-wavelength region (400-500 nm), suggesting thickness-dependent optical behavior. The absorbance then sharply decreased further across the longer wavelengths of the visible range before gradually declining into the near-infrared (NIR) region [39], [40]. This behavior indicates that thicker films tend to be more transparent at higher wavelengths, which could be due to improved crystallinity and reduced scattering. The absorbance of the thinnest film, measuring 250 nm, was higher than that of the thicker films and gradually decreased from the shorter wavelengths in the visible spectrum toward the near-infrared region. The observed reduction in optical absorbance with increasing precursor thickness (250, 300 and 350 nm) may be assigned to enhanced film densification, which decreases photon scattering centers and consequently lowers light absorption [33]. Optical transmittance spectra (Fig. 5) were derived from absorbance measurements using the fundamental relationship [41], [42]:

$$A = 2 - \log 10\ (\%\ T). \quad (1)$$

The transmittance (T) spectra exhibited a noticeable decrease as the film thickness increased. This reduction can be attributed to the enhanced light absorption and scattering within thicker films, which limits the amount of light passing through the material [43], [44].

The absorption coefficient (α) is evaluated via the fundamental relationship [45], [46]:

$$\alpha = \ln (1/T)/t. \quad (2)$$

Figure 6 illustrates that the absorption coefficient (α) increases as the doping concentration rises. This trend is explained by the inverse relationship between the absorption coefficient and transmittance values, as described by (2). As doping concentration increases, the material absorbs more light, reducing transmittance and consequently raising the absorption coefficient [47], [48]. This behavior suggests that higher doping levels enhance the film's ability to interact with and absorb incident light.

The energy gap (E_g)is calculated via (3) [49], [50]:

$$(\alpha h\nu) = A\left(h\nu - E_g\right)^{\frac{1}{2}} . \quad (3)$$

Where $(\alpha h\upsilon)^2$ against incident photon energy ($h\upsilon$), Figure 7 reveals a systematic reduction in E_g from 2.58 eV to 2.43 eV as film thickness increases to 350 nm, demonstrating thickness-dependent band structure modification. This behavior is attributed to the formation of sub-levels within the bandgap, which effectively reduce the overall energy gap [39], [51]. These sub-levels can arise from defects, impurities, or structural changes in thicker films, leading to a narrowing of the bandgap. The observed bandgap narrowing (2.58 to 2.43 eV) directly enhances the material's photoresponse in the visible spectrum, while the reduced carrier effective mass improves electrical.

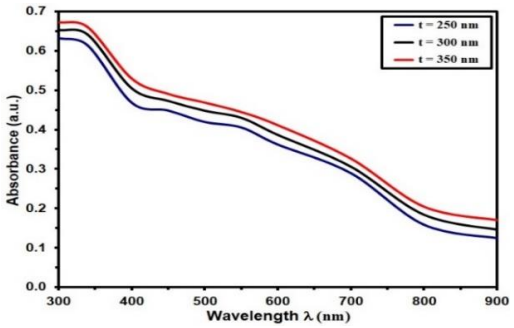

Figure 4: A of the synthesized films.

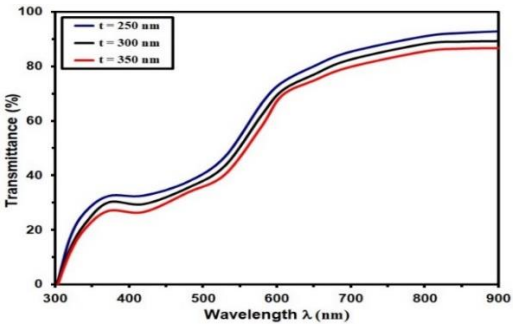

Figure 5: T of the synthesized films.

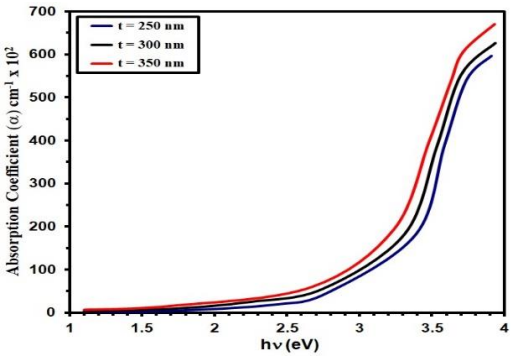

Figure 6: α of the prepared films.

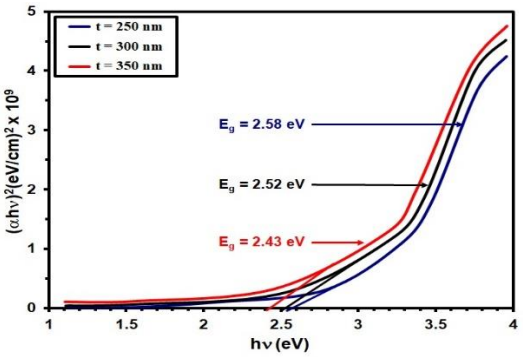

Figure 7: E_g of CdO with different thicknesses.

The extinction coefficient (k) determined via the fundamental optical relation [52], [53]:

$$K = \frac{\alpha\lambda}{4\pi}. \quad (4)$$

Figure 8 illustrates the change of k via wavelength. A rapid decrease in k is observed between 500 nm and 700 nm. The low values of k indicate that the film surface is smooth and homogeneous [54], [55]. This is because k is related to the amount of light absorbed and scattered by the film; lower k values suggest minimal scattering and absorption losses, which are typically associated with uniform and well-ordered film surfaces. Such optical properties are desirable for applications requiring high transparency and minimal surface defects.

The refractive index (n) was calculated via optical reflectance (R) bt (5) [56], [57]:

$$n = \frac{1 + R^{\frac{1}{2}}}{1 - R^{\frac{1}{2}}}. \quad (5)$$

Figure 9 presents the wavelength-dependent refractive index dispersion for all film thicknesses (250-350 nm), revealing significant optical anisotropy correlated with deposition parameters. A noticeable shift of the maximum (n) value toward higher wavelengths is observed with increasing film thickness. This shift is assigned to changes in the film's microstructure and density as thickness increases, which affect how light interacts with the material [58], [59].

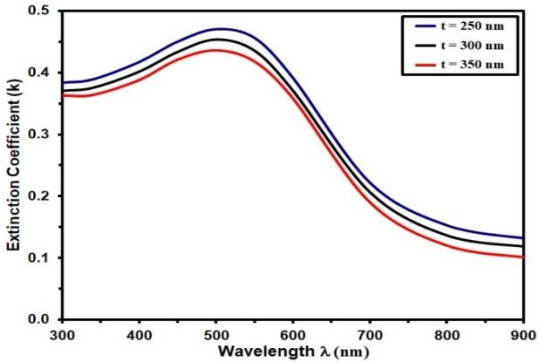

Figure 8: k of the deposit films.

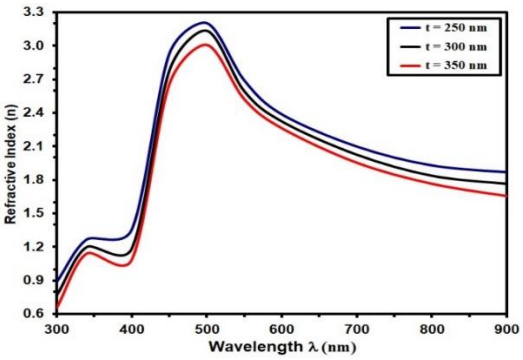

Figure 9: n for deposit films.

The detection sensitivity was evaluated using a standard relation based on the relative change in electrical resistance between the gas-exposed and reference states [60], [61].

In Figure 10, the relationship between time and resistance for cadmium oxide films with different thicknesses (250, 300, and 350 nm) at 225 ppm is presented. The sensor was operated at a temperature of 150°C. When exposed to nitrogen dioxide molecules, oxidation reactions occur on the film surface [62]. During this process, adsorbed oxygen species release trapped electrons back into the conduction band. As a result, the electrical resistance increases, and a higher potential barrier is formed at the grain boundaries [63], [64].

It was also observed that the film with a thickness of 350 nm exhibited the highest resistance response among all samples [65], [66].

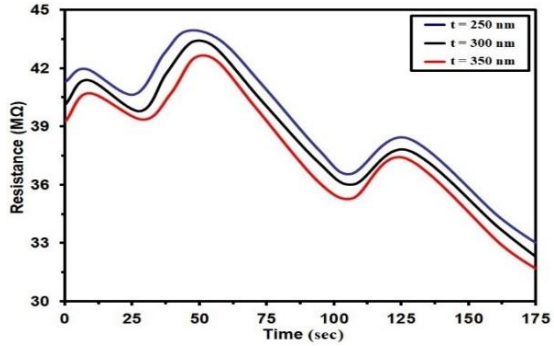

Figure 10: Resistance via time of CdO thin film at 300 ppm NO_2.

The sensitivity curves depicted in Figure 11 showcase how the thickness of CdO films (250, 300, and 350 nm) affects their response to to NO_2 exposure. The sensitivity is greatly affected by the mechanism of recombination among charge carriers, with a noticeable decrease as the thickness increases [67], [68]. Across the range of thicknesses (250, 300, and 350) nm, sensitivity dropped from 23.9 % to 6.0 % (75 ppm), 26.29 % to 8.2 % (150 ppm), and 28.1 % to 10.8 % (250 ppm). This diminishing sensitivity can be attributed to the decrease in surface-to-volume ratio as the CdO film thickness increases, resulting in fewer active sites available for gas interaction [69], [70].

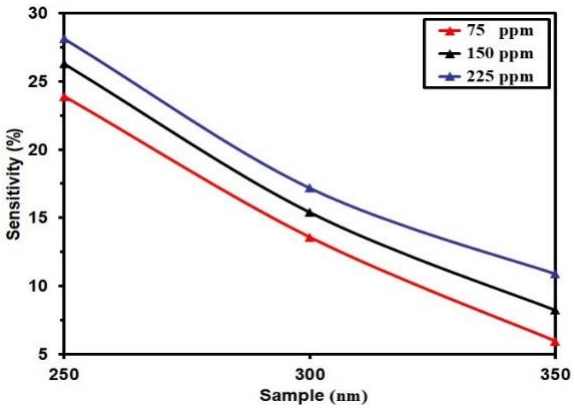

Figure 11: sensitivity (S) versus operating time of CdO thin films.

4 CONCLUSIONS

A simple Spray Pyrolysis process was employed to create CdO with thicknesses of (250, 300, and 350) nm. XRD study revealed that all films have polycrystalline structures and are in the main orientation in the (200) plane. The grain size of CdO with thicknesses of (250, 300, and 350) nm are 10,90, 11,67 and 12,75 nm, respectively, whereas the strain (%) parameter is 3186, 29,69 and 27,19. SEM images show decreased grain size and compact structure in thicker CdO films, with morphology variations due to lattice defects. Thinner films demonstrated better optical absorption and superior NO_2 gas sensitivity. The energy gap was in the field of 2.58 to 2.43 eV in CdO with thicknesses of (250 and 350) nm films, while n and k decreased as thicknesses increased. The optimal performance, especially for gas sensing applications, was achieved at a film thickness of 250 nm. These findings suggest that controlling film thickness is essential for optimizing CdO thin films in many uses like gas sensors and optoelectronic devices.

ACKNOWLEDGMENTS

The authors express their sincere appreciation to Mustansiriyah University, Baghdad, Iraq (www. uomustansiriyah.edu.iq).

REFERENCES

[1] R. Kumaravel, K. Ramamurthi, and V. Krishnakumar, “Effect of indium doping in CdO thin films prepared by spray pyrolysis technique,” J. Phys. Chem. Solids, vol. 71, no. 11, pp. 1545-1549, 2010.

[2] F. P. Koffyberg, “Diffusion of donors in semiconducting CdO,” Solid State Commun., vol. 9, pp. 2187-2189, 1971.

[3] F. Yakuphanoglu, “Preparation of nanostructure Ni doped CdO thin films by sol-gel spin coating method,” J. Sol-Gel Sci. Technol., vol. 59, pp. 569-573, 2011.

[4] R. L. Mishra, A. K. Sharma, and S. G. Prakash, “Gas sensitivity and characterization of cadmium oxide semiconducting thin film deposited by spray pyrolysis technique,” Digest J. Nanomater. Biostruct., vol. 4, pp. 511-518, 2009.

[5] K. Gurumurugan, D. Mangalraj, and S. K. Narayanandas, “Correlations between the optical and electrical properties of CdO thin films deposited by spray pyrolysis,” Thin Solid Films, vol. 251, pp. 7-9, 1994.

[6] O. Gomezdaza, A. Arias-Carbajal Readigos, J. Campos, M. T. S. Nair, and P. K. Nair, “Substrate spacing and thin-film yield in chemical bath deposition of semiconductor thin films,” Semicond. Sci. Technol., vol. 15, no. 11, pp. 1022-1029, 2000.

[7] D. C. Reynolds, D. C. Look, and B. Jogai, “Optically pumped ultraviolet lasing from CdO,” Solid State Commun., vol. 99, pp. 873-875, 1996.

[8] K. Siraj, Ph.D. dissertation, Inst. Appl. Phys., Johannes Kepler Univ. Linz, Linz, Austria, 2007.

[9] V. Radhika and V. Annamalai, "Antibacterial application of undoped and doped CdO nanocrystalline thin films," J. Environ. Nanotechnol., vol. 8, no. 2, pp. 1-10, 2019.

[10] F. G. Hone and T. Abza, "Short review of factors affecting chemical bath deposition method for metal chalcogenide thin films," Int. J. Thin Film Sci. Technol., vol. 8, no. 2, pp. 43-52, 2019.

[11] A. Ashok, G. Regmi, A. Romero-Núñez, M. Solis-López, S. Velumani, and H. Castaneda, "Comparative studies of CdS thin films by chemical bath deposition techniques as a buffer layer for solar cell applications," J. Mater. Sci. Mater. Electron., vol. 31, pp. 7499-7518, 2020.

[12] Shameem, P. Devendran, V. Siva, M. Raja, S. Asath Bahadur, and A. Manikandan, "Preparation and characterization studies of nanostructured CdO thin films by SILAR method for photocatalytic applications," J. Inorg. Organomet. Polym., vol. 27, pp. 692-697, 2017.

[13] M. Rajini, M. Karunakaran, and K. Kasirajan, "An investigation of SILAR grown CdO thin films," Mater. Sci. Poland, vol. 37, no. 1, pp. 25-32, 2019.

[14] H. Güney and D. İskenderoğlu, "The effect of Zn doping on CdO thin films grown by SILAR method at room temperature," Physica B Condens. Matter, vol. 552, pp. 119-123, 2019.

[15] A. A. Dakhel and F. Z. Henari, "Optical characterization of thermally evaporated thin CdO films," Cryst. Res. Technol., vol. 38, pp. 979-985, 2003.

[16] Z. Zhao, D. L. Morel, and C. S. Ferekides, "Electrical and optical properties of tin-doped CdO films deposited by atmospheric metalorganic chemical vapor deposition," Thin Solid Films, vol. 413, pp. 203-211, 2002.

[17] R. K. Gupta, K. Ghosh, R. Patel, and P. K. Kahol, "Highly conducting and transparent Ti-doped CdO films by pulsed laser deposition," Appl. Surf. Sci., vol. 255, pp. 6252-6255, 2009.

[18] K. Z. Yahya and M. Adel, "Influence of substrate temperature on structure and optical properties of CdO thin films prepared by pulsed laser deposition," Eng. Tech. J., vol. 30, pp. 416-425, 2012.

[19] Q. Zhou, Z. Ji, B. B. Hu, C. Chen, L. Zhao, and C. Wang, "Low resistivity transparent conducting CdO thin films deposited by DC reactive magnetron sputtering at room temperature," Mater. Lett., vol. 61, pp. 531-534, 2007.

[20] Y. Yang et al., "CdO as the archetypical transparent conducting oxide: Systematics of dopant ionic radius and electronic structure effects on charge transport and band structure," J. Am. Chem. Soc., vol. 127, pp. 8796-8804, 2005.

[21] A. W. Metz et al., "Transparent conducting oxides: Texture and microstructure effects on charge carrier mobility in MOCVD-derived CdO thin films grown with a thermally stable, low-melting precursor," J. Am. Chem. Soc., vol. 126, pp. 8477-8492, 2004.

[22] S. Jin et al., "Tuning the properties of transparent oxide conductors: Dopant ion size and electronic structure effects on CdO-based transparent conducting oxides," J. Am. Chem. Soc., vol. 126, pp. 13787-13793, 2004.

[23] T. K. Subramanyam, S. Uthanna, and B. Srinivasulu Naidu, "Studies on dc magnetron sputtered cadmium oxide films," Appl. Surf. Sci., vol. 169-170, pp. 529-534, 2001.

[24] J. Santos Cruz, G. Torres Delgado, R. Castanedo Perez, C. I. Zuniga Romero, and O. Zelaya Angel, "Optical and electrical characterization of fluorine doped cadmium oxide thin films prepared by the sol-gel method," Thin Solid Films, vol. 515, pp. 5381-5385, 2007.

[25] P. K. Ghosh, R. Maity, and K. K. Chattopadhyay, "Electrical and optical properties of highly conducting CdO:F thin film deposited by sol-gel dip coating technique," Sol. Energy Mater. Sol. Cells, vol. 81, pp. 279-289, 2004.

[26] Sahin, Y. Gulen, F. Bayansal, H. A. Cetinkara, and H. S. Guder, "Structural and optical properties of Ba-doped CdO films prepared by SILAR method," Superlattices Microstruct., vol. 65, pp. 56-63, 2014.

[27] S. S. Chiad and T. H. Mubarak, "The effect of Ti on physical properties of Fe2O3 thin films for gas sensor applications," Int. J. Nanoelectron. Mater., vol. 13, no. 2, pp. 221-232, 2020.

[28] S. Aksoy, Y. Caglar, S. Ilican, and M. Caglar, "Effect of heat treatment on physical properties of CdO films deposited by sol-gel method," Int. J. Hydrogen Energy, vol. 34, pp. 5191-5195, 2009.

[29] H. Bhosale, A. V. Kambale, A. V. Kokate, and K. Y. Rajpure, "Structural, optical and electrical properties of chemically sprayed CdO thin films," Mater. Sci. Eng. B, vol. 122, pp. 67-71, 2005.

[30] B. A. Bader, S. K. Muhammad, A. M. Jabbar, K. H. Abass, S. S. Chiad, and N. F. Habubi, "Synthesis and characterization of indium-doped CdO nanostructured thin films: A study on optical, morphological, and structural properties," J. Nanostruct., vol. 10, no. 4, pp. 744-750, 2020.

[31] O. Niitsoo et al., "Chemical bath deposited CdS/CdSe-sensitized porous TiO_2 solar cells," J. Photochem. Photobiol. A, vol. 181, pp. 306-313, 2006.

[32] M. Ortega, G. Santana, and A. Morales-Acevedo, "Optoelectronic properties of CdO/Si photodetectors," Solid State Electron., vol. 44, p. 1765, 2000.

[33] M. H. Albanda Al-Timimi, W. H. Abdullah, and M. Z., "Influence of thickness on some physical characterization for nanostructured MgO thin films," East Eur. J. Phys., vol. 2, pp. 173-181, 2023.

[34] R. S. Ali, M. K. Mohammed, A. A. Khadayeir, Z. M. Abood, N. F. Habubi, and S. S. Chiad, "Structural and optical characterization of sprayed nanostructured indium doped Fe2O3 thin films," J. Phys. Conf. Ser., vol. 1664, no. 1, 2020.

[35] M. Ortega, G. Santana, and A. Morales-Acevedo, "Optoelectronic properties of CdO-Si heterojunctions," Superficies Vacio, vol. 9, p. 294, 1999.

[36] F. A. Benko and F. P. Koffyberg, "Quantum efficiency and optical transitions of CdO photoanodes," Solid State Commun., vol. 57, p. 901, 1986.

[37] S. P. Desai, M. P. Suryawanshi, S. M. Bhosale, J. H. Kim, and A. V. Moholkar, "Influence of growth temperature on the physico-chemical properties of sprayed cadmium oxide thin films," Ceram. Int., vol. 41, pp. 4867-4873, 2015.

[38] N. O. Ongwen, A. O. Oduor, and E. O. Ayieta, "Effect of deposition temperature on the optical properties of iron doped cadmium stannate thin films deposited by spray pyrolysis," IJSTRE, vol. 4, no. 3, 2019.

[39] H. Hadi, M. A. Abbsa, A. A. Khadayeir, Z. M. Abood, N. F. Habubi, and S. S. Chiad, "Effects of Mn doping on the characterization of nanostructured TiO2 thin films deposited via chemical spray pyrolysis method," J. Phys. Conf. Ser., vol. 1664, no. 1, 2020.

[40] R. K. Gupta, K. Ghosh, R. Patel, S. R. Mishra, and P. K. Kahol, "Preparation and characterization of highly conducting and transparent Al doped CdO thin films by pulsed laser deposition," Curr. Appl. Phys., vol. 9, pp. 673-677, 2009.

[41] A. A. Dakhel, "Transparent conducting properties of samarium-doped CdO," J. Alloys Compd., vol. 475, pp. 51-54, 2009.

[42] L. R. de León-Gutiérrez, J. J. Cayente-Romero, J. M. Peza-Tapia, E. Barrera-Calva, J. C. Martínez-Flores, and M. Ortega-López, "Some physical properties of Sn-doped CdO thin films prepared by chemical bath deposition," Mater. Lett., vol. 60, pp. 3866-3870, 2006.

[43] A. A. Khadayeir, R. I. Jasim, S. H. Jumaah, N. F. Habubi, and S. S. Chiad, "Influence of substrate temperature on physical properties of nanostructured ZnS thin films," J. Phys. Conf. Ser., vol. 1664, no. 1, 2020.

[44] R. Kuekha, T. H. Mubarak, and B. Azhdar, "Electromagnetic interference shielding and characterization of Ni2+ substituted cobalt nanoferrites prepared by sol-gel auto combustion," Adv. Mater. Sci. Eng., Art. no. 3992402, 2023.

[45] Akyuz, S. Kose, E. Ketenci, V. Bilgin, and F. Ayata, "Title," J. Alloys Compd., vol. 509, pp. 1947-1952, 2011.

[46] R. S. Rusu and G. I. Rusu, "On the electrical and optical characteristics of CdO thin films," J. Optoelectron. Adv. Mater., vol. 7, no. 2, pp. 823-828, 2005.

[47] S. S. Chiad, A. S. Alkelaby, and K. S. Sharba, "Optical conduct of nanostructure Co3O4 rich highly doping Co3O4:Zn alloys," J. Glob. Pharma Technol., vol. 11, no. 7, pp. 662-665, 2020.

[48] K. L. Chopra and S. R. Das, Thin Film Solar Cells. New York, NY, USA: Plenum Press, 1993.

[49] M. Carballeda-Galicia et al., "High transmittance CdO thin films obtained by the sol-gel method," Thin Solid Films, vol. 371, pp. 105-108, 2000.

[50] J. N. Pankove, Optical Processes in Semiconductors. New York, NY, USA: Dover, 1971.

[51] A. A. Khadayeir, E. S. Hassan, T. H. Mubarak, S. S. Chiad, N. F. Habubi, M. O. Dawood, and I. A. Al-Baidhany, "The effect of substrate temperature on the physical properties of copper oxide films," J. Phys. Conf. Ser., vol. 1294, no. 2, Art. no. 022009, 2019.

[52] S. Bose and A. K. Barua, "The role of ZnO:Al films in the performance of amorphous-silicon based tandem solar cells," J. Phys. D Appl. Phys., vol. 32, no. 3, pp. 213-218, Feb. 1999.

[53] R. K. Gupta, K. Ghosh, R. Patel, S. R. Mishra, and P. K. Kahol, "Structural, optical and electrical properties of In doped CdO thin films for optoelectronic applications," Mater. Lett., vol. 62, pp. 3373-3375, 2008.

[54] J. S. Blakemore, Solid State Physics, 2nd ed. Cambridge, U.K.: Cambridge Univ. Press, 1985.

[55] R. Kuekha, T. H. Mubarak, and B. Azhdar, "Synthesis, structural, magnetic, and dielectric properties of Ni2+, Mn2+ co-substituted CoFe2O4 nanoferrites using sol-gel auto combustion method," Mater. Sci. Eng. B, vol. 292, Art. no. 116411, 2023.

[56] O. Gomez, A. Arias, J. Campos, M. T. S. Nair, and P. K. Nair, "Formation of conductive CdO thin films on photoconductive CdS thin films for window layer applications in solar cells," Mod. Phys. Lett. B, vol. 17, p. 609, 2001.

[57] M. A. Yildirim and A. Ates, "Structural, optical and electrical properties of CdO/$Cd(OH)_2$ thin films grown by the SILAR method," Sens. Actuat. A, vol. 155, pp. 272-277, 2009.

[58] J. Tauc, R. Grigorovici, and A. Vancu, "Optical properties and electronic structure of amorphous germanium," Phys. Status Solidi B, vol. 15, pp. 627-637, 1966.

[59] J. I. Pankove, Optical Processes in Semiconductors. Englewood Cliffs, NJ, USA: Prentice-Hall, 1971.

[60] M. A. Rahman and M. K. R. Khan, "Effect of annealing temperature on structural, electrical and optical properties of spray pyrolytic nanocrystalline CdO thin films," Mater. Sci. Semicond. Process., vol. 24, pp. 26-33, 2014.

[61] Z. Serbetci, B. Gunduz, A. Al-Ghamdi, F. Al-Hazmic, K. Ark, and F. El-Tantawy, "Termination of optical constants of nanocluster CdO thin films deposited by sol-gel technique," Acta Phys. Pol. A, vol. 126, p. 798, 2014. [Online]. Available: http://dx.doi.org/10.12693/APhysPolA.126.798.

[62] D. J. Seo, "Structural and optical properties of CdO films deposited by spray pyrolysis," J. Korean Phys. Soc., vol. 45, pp. 1575-1579, 2004.

[63] E. Simon, A. M. Al-Baldawi, A. H. Fiaem, and K. J. Abd Al-Satter, "Preparation and study characteristics of CdO thin film," J. Al-Nahrain Univ., vol. 12, no. 4, p. 92, 2009.

[64] M. H. Suhail, I. M. Ibrahim, and G. Mohan Rao, "Characterization and gas sensitivity of cadmium oxide thin films prepared by thermal evaporation technique," Int. J. Thin Film Sci. Technol., vol. 1, no. 1, p. 1, 2012.

[65] J. Santos-Cruz, G. Torres-Delgado, and R. Castanedo-Perez, "Dependence of electrical and optical properties of sol-gel prepared undoped cadmium oxide thin films on annealing temperature," Thin Solid Films, vol. 493, p. 83, 2005.

[66] A. M. Ashraf, S. M. J. Akhtar, A. F. Khan, Z. Ali, and A. Qayyum, "Effect of annealing on structural and optoelectronic properties of nanostructured ZnSe thin films," J. Alloys Compd., vol. 509, pp. 2414-2419, 2011.

[67] V. Bilgin, S. Kose, F. Atay, and I. Akyuz, “The effect of substrate temperature on the structural and some physical properties of ultrasonically sprayed CdS films,” Mater. Chem. Phys., vol. 94, pp. 103-108, 2005.

[68] M. Di Giulio, G. Miccci, R. Rella, P. Siciliano, and A. Tepore, “Optical absorption of tellurium suboxide thin films,” Phys. Status Solidi A, vol. 136, pp. K101-K104, 1993.

[69] Z. Zhao, D. L. Morel, and C. S. Ferekides, “Electrical and optical properties of tin-doped CdO films prepared by atmospheric metalorganic chemical vapor deposition,” Thin Solid Films, vol. 413, pp. 203-211, 2002.

[70] R. Chandiramouli and B. G. Jeyaprakash, “Review of CdO thin films,” Solid State Sci., vol. 16, pp. 102-110, 2013.